Annals of Biomedical Engineering, Vol. 33, No. 5, May 2005 (© 2005) pp. 567–576
DOI: 10.1007/s10439-005-4388-9

Fluid-Structure Coupled CFD Simulation of the Left Ventricular Flow During Filling Phase

YONGGUANG CHENG,[1] HERBERT OERTEL,[2] and Torsten Schenkel[2]

[1]State Key Laboratory of Water Resources and Hydropower Engineering Science, Wuhan University, 430072 Wuhan, China and
[2]Institute of Fluid Mechanics, University of Karlsruhe, 76128 Karlsruhe, Germany

(Received 22 June 2004; accepted 1 December 2004)

Abstract—The fluid-structure coupled simulation of the heart, though at its developing stage, has shown great prospect in heart function investigations and clinical applications. The purpose of this paper is to verify a commercial software based fluid-structure interaction scheme for the left ventricular filling. The scheme applies the finite volume method to discretize the arbitrary Lagrangian–Eulerian formulation of the Navier–Stokes equations for the fluid while using the nonlinear finite element method to model the structure. The coupling of the fluid and structure is implemented by combining the fluid and structure equations as a unified system and solving it simultaneously at every time step. The left ventricular filling flow in a three-dimensional ellipsoidal thin-wall model geometry of the human heart is simulated, based on a prescribed time-varying Young's modulus. The coupling converges smoothly though the deformation is very large. The pressure–volume relation of the model ventricle, the spatial and temporal distributions of pressure, transient velocity vectors as well as vortex patterns are analyzed, and they agree qualitatively and quantitatively well with the existing data. This preliminary study has verified the feasibility of the scheme and shown the possibility to simulate the left ventricular flow in a more realistic way by adding a myocardial constitutive law into the model and using a more realistic heart geometry.

Keywords—Fluid-structure interaction, Computational fluid dynamics, Left ventricular filling.

INTRODUCTION

In recent years, the Computational Fluid Dynamics (CFD) simulation of the heart flow has made great progress and has been playing an important role in investigating the heart function. The most active CFD approaches to simulate the heart flow might be roughly classified as three types: geometry-prescribed CFD methods,[1–3,10,14,17,18,22,23,24,27] fictitious Fluid-Structure Interaction (FSI) methods[11,12,15,16,21,28] and realistic FSI methods.[4,29,30,32] The geometry-prescribed CFD method, simulating problems on prescribed moving meshes or boundaries constructed mostly from Computerized Tomography (CT) or Magnetic Resonance Imaging/Tomography (MRI/MRT) data, is a one-way approach, which does not consider the structure's feedback on the fluid. The fictitious FSI method, mainly the immersed boundary method, is a kind of macroscopic approximation approach. The immersed boundary method[21] simplifies the structure to buoyant elastic fibers described as fluid-immersed chains of points and uses a Dirac delta based interpolation function to represent the interaction of fluid and structure. These two types of methods are currently very useful in studies and clinical applications.[10–12,14,22,23] However, the realistic FSI method, modeling the structure by the conventional Finite Element Method (FEM), the fluid by CFD and using more realistic coupling algorithms, is the most profound and promising one. Because only this type of method is hopeful to finally resolve the complex properties of the cardiac structure and the delicate interaction of fluid and structure, and, only this type of method has the prospect to finally achieve the goal of modeling the total heart function by integrating cardiac anatomy, electrical activation, mechanics, metabolism and fluid mechanics together, as in the computational framework proposed by Hunter *et al.*[9] There were several attempts on the realistic FSI simulation of the heart flow. Chahboune *et al.*[4] proposed a FEM based FSI scheme for two-dimensional simulation of the complete cardiac cycle in a simplified model of the left ventricle. Vierendeels *et al.*[29,30] built an axisymmetric two-dimensional FSI model with nonlinear thin-shell theory for the filling of a simplified canine ventricle, and produced reasonable pressure distributions and vortex patterns. In their works, simplified ventricular geometries and wall properties were used. Recently, Watanabe *et al.*[32] presented a three-dimensional FSI model, in which a heart wall constitutive law was introduced into the structure part while the fluid dynamics part was eliminated. Taking the propagation of excitation into account, they simulated the fluid-structure interaction during the human left heart contraction in normal excitement and arrhythmia. The above works promoted

Address correspondence to Dr. Yongguang Cheng, State Key Laboratory of Water Resources and Hydropower Engineering Science, Wuhan University, 430072 Wuhan, China. Electronic mail: chengyg2004@yahoo.com.cn

0090-6964/05/0500-0567/1 © 2005 Biomedical Engineering Society

individual models for FSI simulation of the heart flow, obtained reasonable results, and gave us inspiration, though the topic is still challenging.

A successful realistic FSI heart flow simulation needs, at least, the three aspects below to be reasonably resolved. First, the structure solver must be able to describe the nonlinear, anisotropic and inhomogeneous tissular characteristics of the heart wall. Second, the CFD code must be able to treat the large deformation of flow domains and update the computational meshes accordingly. Third, most importantly, the coupling algorithm must be able to couple the fluid and structure systems correctly and ensure convergence. These require an integrative development of myocardial mechanics, nonlinear FEM, moving mesh CFD, Computational Mesh Dynamics (CMD), as well as FSI algorithm. Fortunately, significant progress has been made. For example, several constitutive laws for the muscular structure of the heart wall were provided;[7,13] a finite element model for analyzing ventricular mechanics was suggested;[9,19] the Arbitrary Lagrangian–Eulerian (ALE) formulation for the Navier–Stokes equations was used successfully in moving mesh CFD and FSI;[25,34] there were simultaneous and staggered fluid-structure coupling algorithms available.[33] Nevertheless, there is no special software available that treats all of the above aspects simultaneously well. However, one may find that the increasing multi-physics simulation power of some commercial software shows potentials to achieve this kind of task.

The purpose of this work is to test a commercial software based realistic FSI simulation scheme for three-dimensional heart flow. After a brief introduction to the basic aspects of the scheme, the FSI simulation results of the left ventricular flow during the filling phase (form the opening to closing of the mitral valves, namely, from point A to point B in Fig. 1) and the FSI characteristics and flow patterns will be analyzed. As a preliminary study, a simplified ellipsoidal heart geometry and a time-varying modulus of elasticity of the wall material are assumed. In the future, however, as long as a constitutive law of the heart wall is introduced and a real heart geometry is built, it will be promoted to a more realistic simulation model of heart flow.

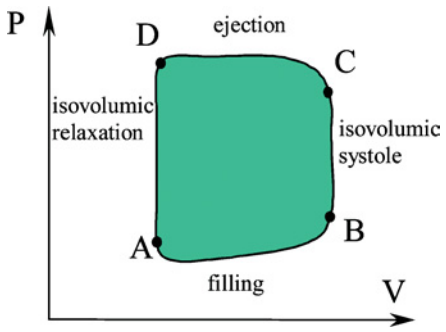

FIGURE 1. Schematic pressure–volume loop of the left ventricle. A to B: filling; B to C: isovolumic systole; C to D: ejection; D to A: isovolumic relaxation.

METHODS

Numerical Scheme

The fundamental conditions applied to the fluid-structure interaction are the kinematic condition (displacement compatibility)

$$\underline{\mathbf{d}}_f = \underline{\mathbf{d}}_s \tag{1}$$

and the dynamic condition (traction equilibrium)

$$\mathbf{n} \cdot \underline{\boldsymbol{\tau}}_f = \mathbf{n} \cdot \underline{\boldsymbol{\tau}}_s \tag{2}$$

where $\underline{\mathbf{d}}_f$ and $\underline{\mathbf{d}}_s$ are, respectively, the fluid and solid displacements. $\underline{\boldsymbol{\tau}}_f$ and $\underline{\boldsymbol{\tau}}_s$ are, respectively, the fluid and solid stresses, and $\mathbf{n}$ stands for the interface normal. The underlining denotes that the values are defined on the fluid-structure interfaces only.

For the fluid flow part, the ALE formulation of Navier–Stokes equations is used, which can be obtained through replacing the convective velocity in the standard Navier–Stokes equations by the relative velocity to the moving mesh. The integral form is as follows

$$\frac{\partial}{\partial t}\int_V \rho\, dV + \int_S \rho(\mathbf{v} - \mathbf{v}_b)\cdot \mathbf{n}\, dS = 0 \tag{3}$$

$$\frac{\partial}{\partial t}\int_V \rho\mathbf{v}\, dV + \int_S (\rho\mathbf{v}(\mathbf{v} - \mathbf{v}_b) + p\mathbf{I} - \boldsymbol{\tau})\cdot \mathbf{n}\, dS = 0 \tag{4}$$

where ρ is the fluid density, $\mathbf{v}$ the velocity vector of fluid in a fixed coordinate system, $\mathbf{v}_b$ the velocity vector of the boundary S of control volume V, $\mathbf{n}$ the normal external to this boundary, p the pressure, $\boldsymbol{I}$ the unit tensor, and $\boldsymbol{\tau}$ the viscous stress tensor. The mesh velocity $\mathbf{v}_b$ must be updated smoothly by a CMD algorithm based on the deformation of flow domains.

When Eqs. (3) and (4) are discretized on the moving mesh by a Finite Volume Method (FVM) scheme, a system of nonlinear equations for fluid can be expressed as

$$\mathbf{F}_f[\mathbf{X}_f, \underline{\mathbf{d}}_s(\mathbf{X}_s)] = 0 \tag{5}$$

in which $\mathbf{X}_f$ and $\mathbf{X}_s$ are the solution vectors for fluid and solid, respectively.

For the solid structure, the FEM is applied to the solid mechanics equations, and yields

$$\mathbf{F}_s[\mathbf{X}_s, \underline{\boldsymbol{\tau}}_f(\mathbf{X}_f)] = 0 \tag{6}$$

It is also a nonlinear equation set for the dynamic and nonlinear material solid system.

Currently available commercial FSI methods include software-software coupling methods (e.g., StarCD coupling PERMAS through MpCCI, CFX coupling ANSYS through MpCCI, etc.) and single-software methods (e.g., FIDAP,

ADINA-FSI, etc.). The latter has better performance than the former for large deformation problems, from the experience of some researchers. In single-software methods, there are two basic types of algorithms for solving the coupled system of equations. One is the iterative method (also called the partitioned or segregated method), in which the fluid equations (5) and the solid equations (6) are solved individually in succession, always using the latest information provided from another part of the coupled system. This iteration is continued until convergence is reached. The other is the direct method (also called the simultaneous method), in which the fluid equations and the solid equations are combined and treated in one system

$$\mathbf{F}[\mathbf{X}] = \begin{bmatrix} \mathbf{F}_f[\mathbf{X}_f, \underline{\mathbf{d}}_s(\mathbf{X}_s)] \\ \mathbf{F}_s[\mathbf{X}_s, \underline{\boldsymbol{\tau}}_f(\mathbf{X}_f)] \end{bmatrix} = 0 \tag{7}$$

and solved simultaneously. Equation (7) may be solved using the Newton–Raphson method.

The direct method for solving the FSI equation system was likely to have better convergence behavior than the iterative one, according to the experience of the authors. In some cases, the direct method could get results while the iterative method was not convergent. However, the direct method needs more computer memory while the iterative method needs much computer time.

Commercial software ADINA-FSI was chosen as the solver of the problem. It applies the above-mentioned scheme and implements several good features. First, the nonlinear and anisotropic material properties could be introduced into the model by the user-defined functions and large deformation nonlinear flexible structures could be simulated, which is important for further simulations of the real heart wall. Second, the Navier–Stokes equations could be solved on ALE meshes, which could be adjusted smoothly by a built-in sub-domain Laplace algorithm, or by prescribed constraints of users according to the movement of boundaries. Third, the coupling scheme could be the direct method or the iterative method, chosen freely by users. The first feature shows a possibility to approximate real heart wall properties, the second ensures the accuracy and stability of the CFD simulation, and the third let the coupling converge fast.

The results of the following simulation are obtained by using the direct coupling method. The iterative method is not convergent for this large deformation problem.

Approach

To simulate the detailed multidimensional flow field of the ventricular filling, we first should ensure that the macroscopic variables defining this process are correct. Therefore, we choose the histories of the intraventricular pressure (P) and transmitral flow velocity (U) during the filling phase of a human heart as the starting point of this simulation, as shown in Fig. 2. The curves were obtained by a lumped parameter model based on the clinical data of a young man. The lumped parameter model, improved from the model by Waite *et al.*[31] is special for modeling diastolic heart.

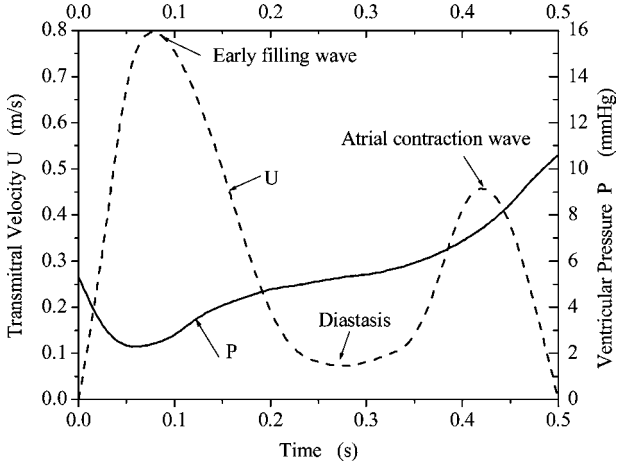

FIGURE 2. Ventricular pressure and transmitral velocity histories of a healthy heart by a lumped model. P: ventricular pressure; U: transmitral velocity.

The main idea of the approach is to get correct spatial and temporal distributions of pressure and velocity within the ventricle by means of fitting the realistic ventricular Pressure–Volume (P–V) loop. The key point is to obtain a fictitious time-varying Young's modulus of the ventricular wall, namely the Young's modulus-time curve. The time-varying modulus of elasticity here is in some way similar to the time-varying elastance of the P–V relation,[26] but their concepts and definitions are different. The time-varying Young's modulus here is just an artifice to approximate the change of ventricular wall mechanical characteristics during the filling, and the applied values of it are related to the model ventricular geometry and wall thickness.

The detailed steps of the approach are explained as follows:

First, by assuming different but temporally constant and spatially uniform Young's moduli and imposing approximate time-varying intraventricular pressures on the model ventricular wall, simulate the ventricle inflation many times by FEM to get a cluster of P–V curves.

Second, based on the above-obtained P–V curves of different Young's moduli, interpolate to get the fictitious Young's modulus-time curve that fits the prescribed P–V curve of the filling phase.

Third, introducing the fictitious Young's modulus-time curve into the heart model and imposing the transmitral velocity history on the mitral orifice position, run the fluid-structure coupled simulation.

Fourth, based on the results of coupled simulations, obtain the relation curve of average intraventricular pressure and ventricular volume and compare it with the target P–V curve, then improve the Young's modulus-time curve until the simulated P–V curve match the target curve.

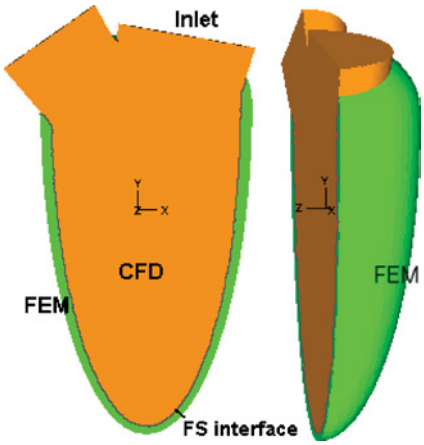

FIGURE 3. Geometry of the model ventricle for the coupled simulation. Green color: ventricular thin wall; orange color: flow domain; inlet: mitral orifice.

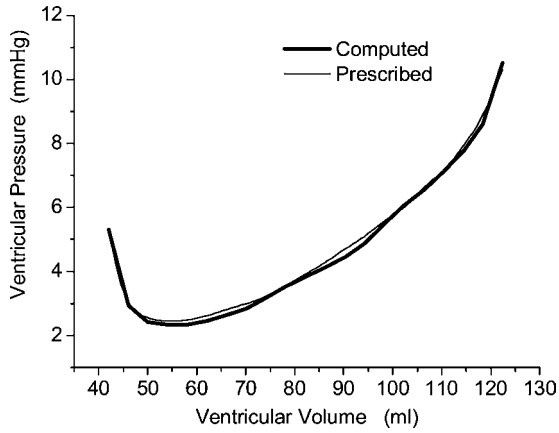

FIGURE 4. Computed ventricular P–V curve comparing with the prescribed one. Bold line: computed; thin line: prescribed.

These procedures, however, should be eliminated in the future work by directly including a realistic myocardial constitutive law.

Simulation Conditions

To simplify the simulation, like most mathematical and numerical analyses, an ellipsoidal thin-wall ventricular model is chosen, as shown in Fig. 3. At the opening moment of the mitral valve, the ventricle diameter on the short axis is 3.6 cm, the ventricle length on the long axis is 7.0 cm, and the wall thickness is 0.2 cm in the basal region and 0.15 cm in the apical region. The inflow passage through the mitral valves is represented by a lean short tube, with a diameter of 2.5 cm in the mitral orifice position. For simplifying problem, the mitral valves are neglected, on which the fluid-structure interaction is much difficult to model. The outflow tract is also simplified as a short tube of diameter 2.1 cm, with a dead end standing for the closed aortic valves. These geometry dimensions are aimed at modeling a normal human heart. Because this geometry has a symmetrical plane ($z = 0$ plane in the coordinates system), only a half of it is selected in the simulation.

The wall material is assumed isotropic and homogeneous, but the nonlinear change of elasticity is taken into account by importing the above-mentioned time-varying Young's modulus into the model. The zero material density is given owing to the very small effect of the wall inertia in this simulation.[7]

The fluid is assumed to be Newtonian, and the density and viscosity are chosen as 1050 kg/m^3, and 0.00316 Pa·s, respectively. They are the normal values of blood. Because the velocity is relatively low (usually <1 m/s) and the normal transmitral blood flow is not fully developed, the laminar model of CFD is applied. The transmitral velocity wave in Fig. 2 is imposed uniformly on the inlet of the model ventricle in the coupled simulation.

In the final simulation, 27,000 and 100,000 tetrahedral elements are generated for the wall and fluid, respectively.

RESULTS AND DISCUSSIONS

Pressure–Volume Relation

Figure 4 shows the simulated P–V curve, of which the typical values are as follows. The chamber volume is about 41.8 ml with a pressure of 5.30 mmHg in the beginning of the filling phase. The volume is 122.3 ml with pressure 10.50 mmHg in the end of the filling phase. The lowest pressure is 2.34 mmHg when the volume is 59 ml. Accordingly, the stroke volume is about 80.5 ml, indicating a very large heart deformation. There is nearly no deviation between the simulated and given volume values because the filling velocity is given. And the largest deviation amplitude in pressures is 0.21 mmHg, which is acceptable. Therefore, generally speaking, the simulated P–V curve fits the prescribed one well, giving us a basic verification of the detailed simulation.

Pressure Distributions

The filling phase is the most important part of the four-phase cardiac cycle (Fig. 1), because it is determinative for the stroke volume.[7] The transmitral velocity history and intraventricular pressure distribution during this phase are the often-used indices to check the overall heart working conditions.[8] The transmitral velocity curve normally has two peaks, as shown in Fig. 2. The first peak is due to ventricular relaxation and is called the Early filling wave (E wave). The second peak is due to atrial contraction and is called the Atrial contraction wave (A wave). Therefore, the filling phase can be divided to three sub-phases: rapid filling phase, slow filling phase (diastasis) and atrial contraction phase.

Figure 5 shows the simulated basal and apical pressures as functions of time. They are the recorded values within

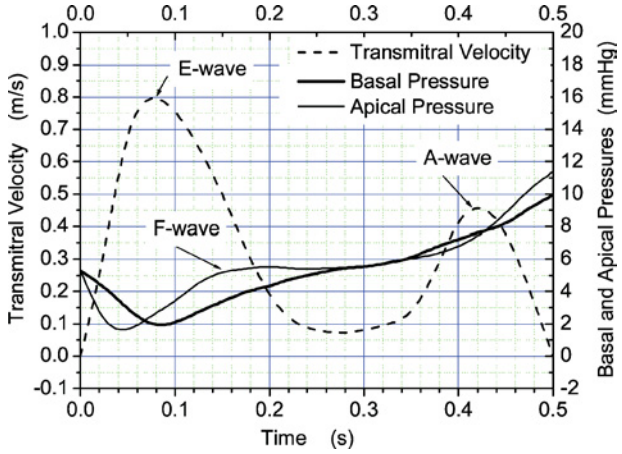

FIGURE 5. Computed histories of basal and apical pressures during the filling. Bold line: basal pressure; thin line: apical pressure; dash line: transmitral velocity.

two CFD elements respectively in the apical and basal locations. It can be seen that, both the basal and apical pressures decrease at first and increase later, approximating the trend of the pressure curve in Fig. 2. The sign of the basal–apical pressure gradient shifts three times: from positive to negative, negative to positive, and positive to negative, consistent with the existing measurements and simulations.[5,6,29,30] Detailedly, during the early period of the rapid filling phase, with the ventriclular enlargement, the total ventricular pressure drops, owing to the continuing relaxation after the isovolumic relaxation. During this period (acceleration), because the filling pressure wave from the base does not reach the apex, the apical pressure is smaller than the basal pressure while they decrease together. Later on, with the progress of rapid filling, the filling pressure wave reaches the apex and the wall gives the filling pressure wave a positive reflection. The superposition of the filling wave and the reflected wave causes a rapid increase of pressure in the apical region, forming a so-called F-wave. Therefore, during the late rapid filling phase (deceleration), the apical pressure becomes larger than the basal pressure. During the slow filling phase, the difference of apical and basal pressures becomes smaller because of the reshape of the ventricle and the redistribution of pressure. Then, during the atrial contraction phase, first the basal pressure increases and becomes larger than the apical pressure, and then when the second filling pressure wave reaches apical region, the apical pressure becomes apparently larger than the basal pressure again. These simulated pressure transmission and reflection phenomena here are in good agreement with the measured and simulated ones.[5,6,29,30] The maximum difference of apical and basal pressures here is about 2.0 mmHg, occurred near the maximum acceleration and deceleration parts of the rapid filling and consistent well with the values (about 2.0–2.5 mmHg) of Vierendeels *et al.*[29] and Ebbers *et al.*[6] Analyzing this phenomenon based on this figure and the existing works,[5,6,20,29,30] one may come to the following conclusions. The intraventricular pressure change is due to the continuing relaxation of ventricular wall and the two filling waves. The continued myocardial relaxation causes the left ventricular pressure to be below the left atrial pressure that leads to the rapid filling, and the relaxation also generates a portion of basal–apical pressure gradient during the early rapid filling, due to the nonuniform deformation of the wall.[20] The contraction of left atrium generates another atrial-ventricular pressure gradient that causes the second filling. The accelerations of the E-wave and A-wave are caused respectively by ventricular relaxation and atrial contraction, while the decelerations are due to the reaction of the ventricular wall to the inflow. Generally, when the filling waves accelerate, the basal pressure is larger than apical pressure, when the waves decelerate the apical pressure overruns the basal pressure. The pressure balance moments are corresponding approximately to the occurrences of the extrema of inflow waveform, reflecting the exchanging process between dynamic energy and potential energy of the fluid in the chamber.

Figure 6 shows the pressure spatial contours on the symmetrical plane ($z = 0$ plane) at several typical moments (corresponding to acceleration, deceleration and peak of E-wave and A-wave, etc.). Apart from showing the propagation of pressure, the detailed pressure distribution also indicates the vortex locations where the pressures are locally lower than in surrounding regions. Apparently, two vortices downstream the mitral orifice are generated by the rapid filling and move longitudinally towards the apical region, along with the enlargement of the ventricle.

Flow Patterns

Figure 7 shows the velocity distributions at several typical moments: the beginning moment of the filling phase, the peak velocity moment of E-wave, the lowest velocity moment of diastasis, the peak velocity moment of A-wave, a large deceleration moment of A-wave, and the end moment of the filling phase. Based on these figures as well as those in the supplementary flow pattern films, the transient flow structure pictures can be described as follows. During the rapid filling phase, a strong filling jet generates and goes from the mitral orifice to the ventricular chamber. Driven by this jet, an annular vortex is formed in the base region downstream the mitral orifice. With the progress of the rapid filling, this first vortex ring travels smoothly towards the middle of the expanding ventricle, as a accessorial consequence, a weak vortex within the aortic outflow tract is formed during the deceleration period. Later on, during the diastasis, the vortex ring reaches the middle of the enlarging ventricle and the posterior side of it goes forward while the anterior side backward. At the same time, the weak vortex enlarges and moves out off the outflow tract, thereby is destroyed in the late diastasis by the inflow stream. Then,

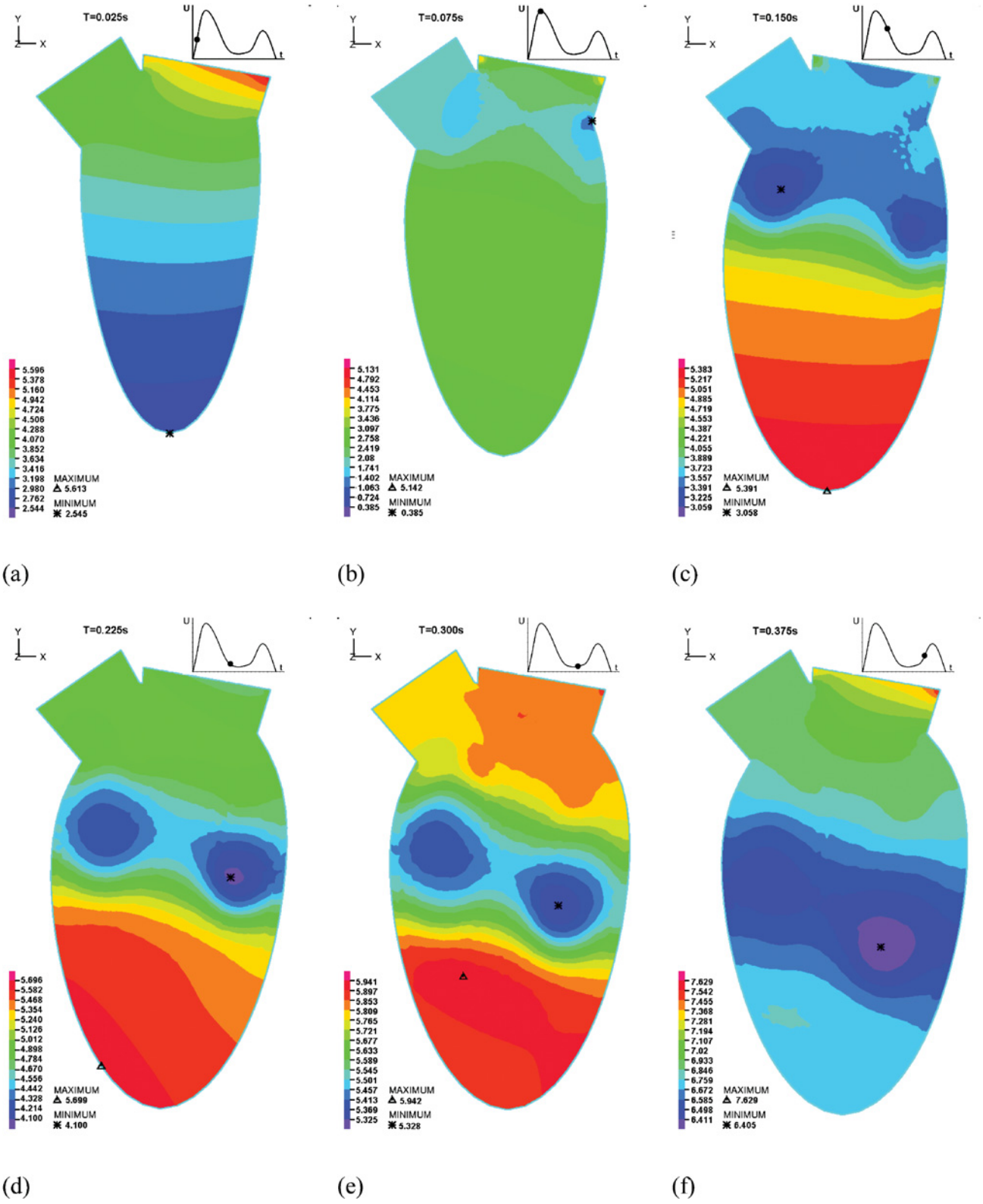

FIGURE 6. Pressure contours of several typical moments during the filling. (a) a large acceleration moment of E-wave; (b) the peak velocity moment of E-wave; (c) a large deceleration moment of E-wave; (d) the beginning moment of diastasis; (e) the lowest velocity moment of diastasis; (f) a large acceleration moment of A-wave; (g) the peak velocity moment of A-wave; (h) a large deceleration moment of A-wave; (i) the end moment of the filling. Every color scale bar is corresponding to its moment.

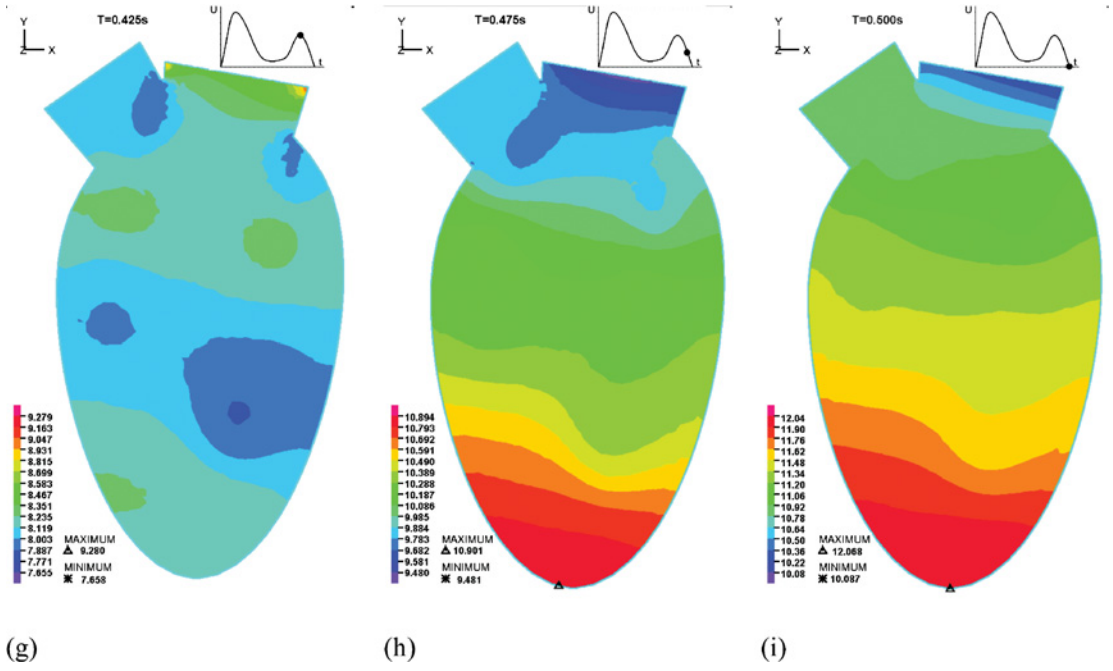

FIGURE 6. Continued.

during the atrial contraction phase, because of the second filling jet, a new but relatively weak vortex ring, with its anterior side in the outflow tract, is generated, while the posterior side of the first vortex ring goes further to the posterior apical region of the chamber. And finally, in the end of the filling, the posterior side of the second vortex ring goes down and partially merges into the first one, forming a final picture in the $z = 0$ plane: a large vortex dominates

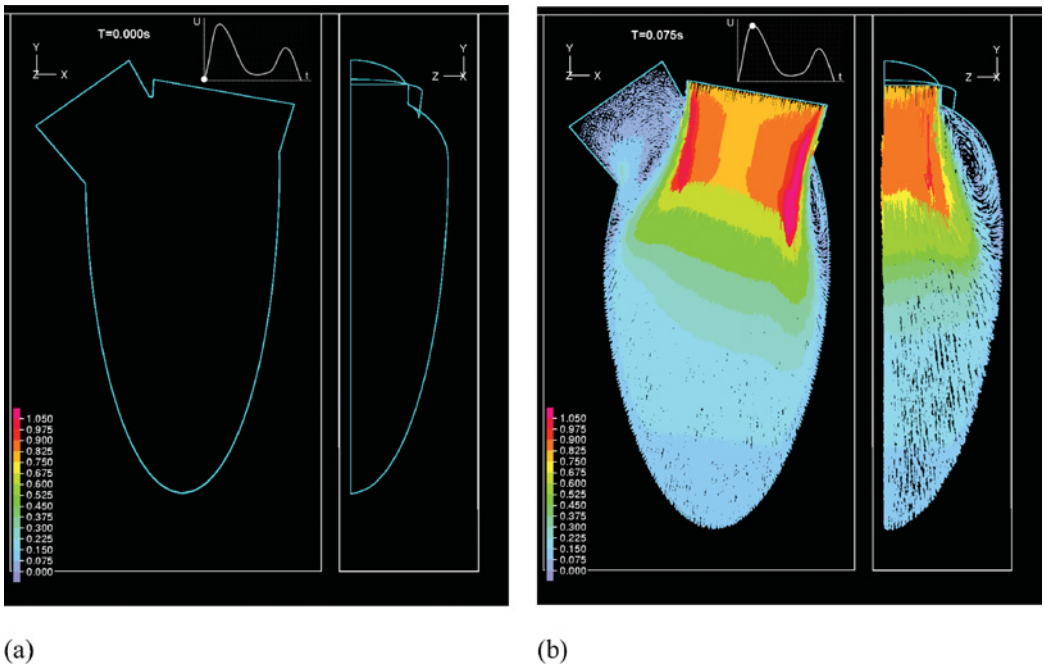

FIGURE 7. Velocity vectors at several typical moments during the filling. (a) the beginning moment of the filling; (b) the peak velocity moment of E-wave; (c) the lowest velocity moment of diastasis; (d) the peak velocity moment of A-wave; (e) a large deceleration moment of A-wave; (f) the end moment of the filling.

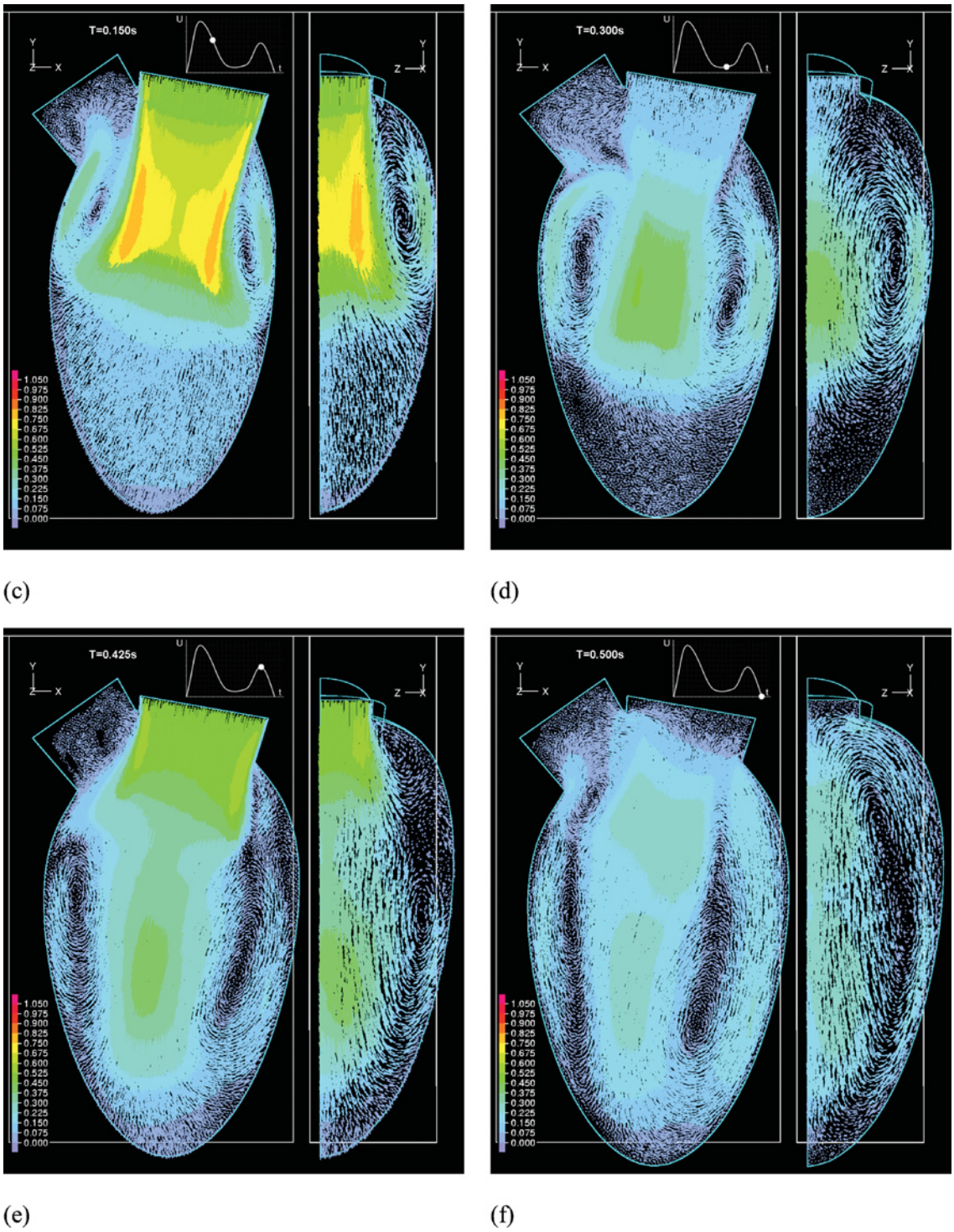

FIGURE 7. Continued.

the posterior apical portion of the ventricle, a second large vortex remains in the anterior middle region and a third vortex exits near the outflow tract. These vortex forming and moving phenomena are generally similar to those of the simulations[1–3,10,17,18,22,23] and measurements.[5,6] The generation and movement of the first vortex ring during the rapid filling fit the existing works very well. However, among these works the detailed patterns during the late diastole are not always consistent owing to different computational and experimental conditions.

CONCLUSIONS

This work mainly focused on investigating the feasibility of the fluid-structure interaction scheme for the heart flow. It was a preparation for further simulations concerning the real heart structure and properties. This commercial software based FSI scheme has some good features in integrality and efficiency for the developing total heart model, which aims at incorporating FEM, CFD, FSI, myocardial mechanics and myocardial activation integrally. The scheme was outlined briefly and the approaches for the ventricular filling simulation were introduced. In the simulation of a simplified human ventricular model, the pressure–volume relation of the model ventricle during filling phase, the velocity and pressure distributions and vortex patterns were analyzed. Reasonable results are obtained, which generally agree well with the previously published simulations and measurements, and are of value for furthering the understanding of the ventricular flow structure.

The simplifications of this simulation, such as thin-wall ventricular geometry, isotropic and homogeneous material, neglecting the mitral valve and imposing uniform inflow velocity, obviously may limit the actual clinical uses. However, the work has validated the large-deformation coupling ability of the scheme and provided us confidence in the future modeling of real heart filling, which may be achieved straightforwardly by introducing a myocardial constitutive law into the FEM model and adopting a real heart geometry. In addition, the present scheme may be used reasonably to explore the relationship of the flow characteristics and ventricular properties, for example, regional ischemia and tachycardia. The ischemia may be modeled by dividing the heart wall to many regions and giving different elasticity coefficients to different regions. The tachycardia can be simulated by changing the time-varying characteristic of elasticity.

ACKNOWLEDGMENTS

Yongguang Cheng is grateful to the State Key Laboratory of Water Resources and Hydropower Engineering Science of Wuhan University and the Institute of Fluid Mechanics of the University of Karlsruhe for supporting and hosting his visiting study in Germany.

REFERENCES

[1]Baccani, B., F. Domenichini, G. Pedrizzetti, and G. Tonti. Fluid dynamics of the left ventricular filling in dilated cardiomyopathy. *J. Biomech.* 35(5):665–671, 2002a.

[2]Baccani, B., F. Domenichini, and G. Pedrizzetti. Vortex dynamics in a model left ventricle during filling. *Eur. J. Mech. B/Fluids* 21:527–543, 2002b.

[3]Baccani, B., F. Domenichini, and G. Pedrizzetti. Model and influence of mitral valve opening during the left ventricular filling. *J. Biomech.* 36:355–361, 2003.

[4]Chahboune, B., and J. M. Crolet. Numerical simulation of the blood-wall interaction in the human left ventricle. *Eur. Phys. J. – Appl. Phys.* 2:291–297, 1998.

[5]Courtois, M., S. J. Kovacs, Jr., and P. A. Ludbrook. Transmitral pressure-flow velocity relation: Importance of regional pressure gradients in the left ventricle during diastole. *Circulation* 78:661–671, 1988.

[6]Ebbers, T., L. Wigström, A. F. Bolger, B. Wranne, and M. Karlsson. Noninvasive measurement of time-varying three-dimensional relative pressure fields within the human heart. *J. Biomech. Eng.* 124:288–293, 2002.

[7]Fung, Y. C. Biomechanics: Circulation. 2nd ed. Berlin, Heidelberg, New York: Springer, 1997.

[8]Gibson, D. G., and D. P. Francis. Clinical assesment of left ventricular diastolic function. *Heart* 89:231–238, 2003.

[9]Hunter, P. J., A. J. Pullan, and B. H. Smaill. Modeling total heart function. *Annu. Rev. Biomed. Eng.* 5:147–177, 2003.

[10]Keber, R. Computational fluid dynamics simulation of human left ventricular flow. PhD Dissertation, University of Karlsruhe, Karlsruhe. (In German), 2003.

[11]Lemmon, J. D., and A. P. Yoganathan. Three-dimensional computational model of left heart diastolic function with fluid-structure interaction. *J. Biomech. Eng.* 122:109–117, 2000a.

[12]Lemmon, J. D., and A. P. Yoganathan. Computational modeling of left heart diastolic function: Examination of ventricular dysfunction. *J. Biomech. Eng.* 122:297–303, 2000b.

[13]Lin, D. H. S., and F. C. P. Yin. A multiaxial constitutive law for mammalian left ventricular myocardium in steady-state barium contracture or tetanus. *J. Biomech. Eng.* 120:504–517, 1998.

[14]Long, Q., R. Merrifield, G. Z. Yang, X. Y. Xu, P. J. Kilner, and D. N. Firman. The influence of inflow boundary conditions on intra left ventricle flow predictions. *J. Biomech. Eng.* 125:922–927, 2003.

[15]McQueen, D. M., and C. S. Peskin. Shared-memory parallel vector implementation of the immersed boundary method for the computation of blood flow in the beating mammalian heart. *J. Supercomput.* 11(3):213–236, 1997.

[16]McQueen, D. M., and C. S. Peskin. A three-dimensional computer model of the human heart for studying cardiac fluid dynamics. *Comput. Graph.* 34:56–60, 2000.

[17]Nakamura, M., S. Wada, T. Mikami, A. Kitabatake, and T. Karino. A computational fluid mechanical study on the effects of opening and closing of the mitral orifice on a transmitral flow velocity profile and an early diastolic intraventricular flow. *JSME Int. J. Ser. C – Mech. Syst. Mach. Elem. Manufact.* 45:913–922, 2002.

[18]Nakamura, M., S. Wada, T. Mikami, A. Kitabatake, and T. Karino. Computational study on the evolution of an intraventricular vortical flow during early diastole for the interpretation of color M-mode Doppler echocardiograms. *Biomech. Model. Mechanobiol.* 2:59–72, 2003.

[19]Nash, M. P., and P. J. Hunter. Computational mechanics of the heart: From tissue structure to ventricular function. *J. Elast.* 61(1/3):113–141, 2000.

[20]Nikolic, S. D., M. P. Feneley, O. E. Pajaro, J. S. Rankin, and E. L. Yellin. Origin of regional pressure gradients in the left ventricle during early diastole. *Am. J. Physiol.-Heart Circulatory Physiol.* 37(2):H550–H557, 1995.

[21]Peskin, C. S., and D. M. McQueen. Fluid dynamics of the heart and its valves, case studies in mathematical modeling. In: Ecology, Physiology and Cell Biology, edited by H. G. Othmer. New Jersey: Prentice-Hall, 1996, pp. 309–337.

[22]Saber, N. R., A. D. Gosman, N. B. Wood, P. J. Kilner, C. L. Charrier, and D. N. Firmin. Computational flow modeling of the

left ventricle based on in vivo MRI data: Initial experience. *Ann. Biomed. Eng.* 29(4):275–283, 2001.

[23] Saber, N. R., N. B. Wood, A. D. Gosman, R. D. Merrifield, G. Z. Yang, C. L. Charrier, P. D. Gatehouse, and D. N. Firmin. Progress towards patient-specific computational flow modeling of the left heart via combination of magnetic resonance imaging with computational fluid dynamics. *Ann. Biomed. Eng.* 31(1):42–52, 2003.

[24] Schoephoerster, R. T., C. L. Silva, and G. Ray. Evaluation of ventricular function based on simulated systolic flow dynamics computed from regional wall motion. *J. Biomech.* 27:125–136, 1994.

[25] Souli, M., A. Ouahsine, and L. Lewin. ALE formulation for fluid-structure interaction problems. *Comput. Methods Appl. Mech. Eng.* 190(5–7):659–676, 2001.

[26] Sunagawa, K., and K. Sagawa. Models of ventricular contraction based on time-varying elastance. *Crit. Rev. Biomed. Eng.* 7:193–288, 1982.

[27] Taylor, T. W., H. Okino, and T. Yamaguchi. Three-dimensional analysis of left ventricular ejection using computational fluid dynamics. *J. Biomech. Eng.* 116:127–130, 1994.

[28] Vesier, C., J. D. Lemmon, R. A. Levine, and A. P. Yoganathan. A three-dimensional computational model of a thin-walled left ventricle. In: Proceedings on IEEE Supercomputing '92, 16–20 November, pp. 73–82, 1992.

[29] Vierendeels, J. A., K. Riemslagh, and E. Dick. Computer simulation of intraventricular flow and pressure gradients during diastole. *J. Biomech. Eng.* 122:667–674, 2000.

[30] Vierendeels, J. A., K. Riemslagh, E. Dick, and P. Verdonck. Computer simulation of left ventricular filling flow: Impact study on echocardiograms. *Comput. Cardiol.* 26:177–180, 1999.

[31] Waite, L. R., S. Schulz, G. Szabo, and C. F. Vahl. A lumped parameter model of left ventricular filling—pressure waveforms. *Biomed. Sci. Instrum.* 36:75–80, 2000.

[32] Watanabe, H., T. Hisada, S. Sugiura, J. Okada, and H. Fukunari. Computer simulation of blood flow, left ventricular wall motion and their interrelationship by fluid-structure interaction finite element method. *JSME Int. J. Ser. C – Mech. Syst. Mach. Elem. Manufact.* 45(4):1003–1012, 2002.

[33] Zhang, H., and K. J. Bathe. Direct and iterative computing of fluid flows fully coupled with structures. In: Computational Fluid and Solid Mechanics, edited by K. J. Bathe, Elsevier Science, 2001.

[34] Zhang, Q., and T. Hisada. Analysis of fluid-structure interaction problems with structural bucking and large domain changes by ALE finite element method. *Comput. Methods Appl. Mech. Eng.* 190:6341–6357, 2001.